Title

Combination prophylactic therapy with rifampin increases efficacy against an experimental Staphylococcus epidermidis subcutaneous implant-related infection.

Journal

Antimicrobial Agents and Chemotherapy, 58(4)

Authors

Niska, Jared
Shahbazian, Jonathan
Loftin, Amanda
et al.

Publication Date

2014

DOI

10.1128/AAC.01943-13

Peer reviewed

AAC Journals.ASM.org

Combination Prophylactic Therapy with Rifampin Increases Efficacy against an Experimental *Staphylococcus epidermidis* Subcutaneous Implant-Related Infection

Alexandra I. Stavrakis,[a] Jared A. Niska,[a] Jonathan H. Shahbazian,[b] Amanda H. Loftin,[a] Romela Irene Ramos,[c] Fabrizio Billi,[a] Kevin P. Francis,[d] Michael Otto,[e] Nicholas M. Bernthal,[a] Daniel Z. Uslan,[f] Lloyd S. Miller[b]

Orthopaedic Hospital Research Center (OHRC), UCLA/Orthopaedic Hospital-Department of Orthopaedic Surgery,[a] Division of Dermatology,[c] Division of Infectious Diseases,[f] David Geffen School of Medicine at University of California, Los Angeles (UCLA), Los Angeles, California, USA; Department of Dermatology, Johns Hopkins University School of Medicine, Baltimore, Maryland, USA[b]; PerkinElmer, Inc., Hopkinton, Massachusetts, USA[d]; Pathogen Molecular Genetics Section, Laboratory of Human Bacterial Pathogenesis, National Institute of Allergy and Infectious Diseases, National Institutes of Health, Bethesda, Maryland, USA[e]

The incidence of infections related to cardiac devices (such as permanent pacemakers) has been increasing out of proportion to implantation rates. As management of device infections typically requires explantation of the device, optimal prophylactic strategies are needed. Cefazolin and vancomycin are widely used as single agents for surgical prophylaxis against cardiac device-related infections. However, combination antibiotic prophylaxis may further reduce infectious complications. To model a localized subcutaneous implant-related infection, a bioluminescent strain of *Staphylococcus epidermidis* was inoculated onto a medical-procedure-grade titanium disc, which was placed into a subcutaneous pocket in the backs of mice. *In vivo* bioluminescence imaging, quantification of *ex vivo* CFU from the capsules and implants, variable-pressure scanning electron microscopy (VP-SEM), and neutrophil enhanced green fluorescent protein (EGFP) fluorescence in LysEGFP mice were employed to monitor the infection. This model was used to evaluate the efficacies of low- and high-dose cefazolin (50 and 200 mg/kg of body weight) and vancomycin (10 and 110 mg/kg) intravenous prophylaxis with or without rifampin (25 mg/kg). High-dose cefazolin and high-dose vancomycin treatment resulted in almost complete bacterial clearance, whereas both low-dose cefazolin and low-dose vancomycin reduced the *in vivo* and *ex vivo* bacterial burden only moderately. The addition of rifampin to low-dose cefazolin and vancomycin was highly effective in further reducing the CFU harvested from the implants. However, vancomycin-rifampin was more effective than cefazolin-rifampin in further reducing the CFU harvested from the surrounding tissue capsules. Future studies in humans will be required to determine whether the addition of rifampin has improved efficacy in preventing device-related infections in clinical practice.

Infection represents one of the most serious complications of implanted medical devices and remains a major impediment to successful clinical outcomes (1). Infections associated with cardiac implantable electrophysiological devices (CIED), such as permanent pacemakers (PPMs) or implantable cardioverters-defibrillators (ICDs), are especially problematic as they are particularly difficult to treat and result in increased morbidity and mortality (2–4). Most CIED-related infections involve the surrounding tissues in the subcutaneous pocket, leading to pain, erythema, swelling, and, occasionally, purulent drainage and fistula formation (2–4). However, deep-seated pocket infections can present with nonspecific pain in the pocket without other local or systemic signs of infection, making them difficult to diagnose (2–4). CIED infections can result in life-threatening complications since the bacteria can follow the lead wires to the endocardial surface, leading to endocarditis, septic shock, and pulmonary septic emboli (2–4).

A hallmark of CIED infections (and surgical implant infections in general) is the development of bacterial biofilms on the implanted foreign materials that prevent penetration of immune cells and antibiotics (5, 6). Biofilm infections are exceedingly difficult to treat, and removal and replacement of the infected device, along with prolonged antibiotics, are often necessary to eradicate the infection (1–4). Therefore, preventing an infection at the time of surgical implantation is critical (1–4). Numerous strategies for prophylaxis have been attempted, including intraoperative lavage of the device pocket with an antiseptic or antibiotic solution, direct antibiotic application to the device, and an antibiotic-impregnated mesh coating for the device (1–4, 7–10). However, perioperative intravenous antibiotic prophylaxis has become the mainstay of preventative therapy and has been proven to reduce CIED infections (4, 11–15). Currently, either a first-generation cephalosporin (e.g., cefazolin) or vancomycin is recommended for antibiotic prophylaxis because they provide coverage against staphylococcal species, especially *Staphylococcus epidermidis* and *S. aureus*, which are the causative bacteria in the majority (60% to 80%) of CIED infections (16–20). However, despite enhanced aseptic surgical techniques and the widespread use of antibiotic prophylaxis, the numbers of infections associated with CIED over the past decade have been rising faster than the rate of implantation (21, 22). The reasons for this have been attributed to the increased numbers of CIED implantations in elderly patients and

Received 7 September 2013 Returned for modification 5 December 2013
Accepted 2 February 2014
Published ahead of print 10 February 2014
Address correspondence to Daniel Z. Uslan, duslan@mednet.ucla.edu, or Lloyd S. Miller, lloydmiller@jhmi.edu.
A.I.S. and J.A.N. contributed equally to this article.

doi:10.1128/AAC.01943-13

patients with comorbidities (18, 21, 22). As the demand for CIED continues to grow, optimizing antibiotic prophylaxis strategies may help reduce infectious complications and improve clinical outcomes (2–4). With an infection rate of ~1% for CIED (14, 18), a randomized prospective clinical trial designed to compare efficacies of different prophylactic regimens would take a large number of patients and would thus be extremely costly to perform. Therefore, we set out in this study to develop a preclinical mouse model of a localized CIED infection to evaluate the efficacies of different prophylactic antibiotic therapies before larger studies in humans. This model involved the subcutaneous implantation of a medical-procedure-grade titanium disc inoculated with a *S. epidermidis* bioluminescent strain (23). *In vivo* bioluminescent imaging was employed to monitor the bacterial burden noninvasively and longitudinally over time. In addition, to evaluate the degree of inflammation induced by the infection, LysEGFP mice, which represent a genetically engineered mouse strain that possesses green-fluorescent myeloid cells (mostly neutrophils), were used in combination with *in vivo* fluorescence imaging (24–26). Using this model, the efficacy of cefazolin and vancomycin intravenous prophylaxis was evaluated. In addition, combination prophylactic therapy with rifampin was also investigated, since rifampin can penetrate biofilms (27–30) and rifampin combination therapy is recommended in the treatment regimens for certain surgical implant infections (e.g., orthopedic implant infections and prosthetic valve infections [31, 32]). Moreover, rifampin is included (along with minocycline) in the FDA-approved antibiotic-impregnated mesh to prevent CIED infections (10).

MATERIALS AND METHODS

***S. epidermidis* bioluminescent strain.** The Xen43 *S. epidermidis* strain (PerkinElmer, Hopkinton, MA) used in this study was previously derived from *S. epidermidis* 1457, a clinical isolate from an infected central venous catheter that has established biofilm-producing activity as previously described (23, 33). This strain possesses a stably integrated, modified *luxABCDE* operon from the bacterial insect pathogen *Photorhabdus luminescens* which results in the natural emission of a blue-green light from live and metabolically active bacteria. The construct is integrated into the bacterial chromosome and is thus maintained in all progeny. This strain has been previously used to study biofilm formation in a subcutaneous catheter infection in mice (23).

Preparation of bacteria. Xen43 was streaked onto tryptic soy agar plates (tryptic soy broth [TSB] plus 1.5% Bacto agar [BD Biosciences, Franklin Lakes, NJ]) and grown at 37°C overnight. Single bacterial colonies of Xen43 were cultured in TSB and grown overnight at 37°C in a shaking incubator (MaxQ 420 HP; Thermo Fisher Scientific, Waltham, MA) (240 rpm) in TSB. Mid-logarithmic-phase bacteria were obtained after a 2-h subculture of a 1/50 dilution of the overnight culture. Bacteria were pelleted, resuspended, and washed three times in TSB. Bacterial inocula (1×10^6, 1×10^7, or 1×10^8 CFU/ml TSB) were estimated by measuring the absorbance at 600 nm (Biomate 3; Thermo Fisher Scientific) and verified after overnight culture on plates.

Bacterial inoculation of titanium discs. Medical-procedure-grade titanium discs (Medtronic, Inc., Mounds View, MN) (5 mm in diameter, 0.4 mm thick) (sterilized by autoclaving) were incubated for 30 min with mild shaking at 37°C in TSB containing 1×10^6, 1×10^7, or 1×10^8 CFU of Xen43 or broth alone with no bacteria (uninfected). The discs were thoroughly rinsed with sterile saline solution before being surgically implanted into the mice.

Mice. Eight-week-old male C57BL/6 mice obtained from Jackson Laboratories (Bar Harbor, ME) were used. In some experiments, 8-week-old LysEGFP mice, representing a genetically engineered mouse line on a C57BL/6 background that possesses green-fluorescent myeloid cells due to a knock-in of enhanced green fluorescence protein (EGFP) into the lysozyme M gene, were used (24–26).

Mouse surgical procedures. All procedures were approved by the UCLA Animal Research Committee. To model a localized CIED or other subcutaneous implant-related infection, a small incision was made on the upper dorsal backs of mice and a subcutaneous pocket was made with gentle undermining (Fig. 1). A titanium disc that was incubated with *S. epidermidis* (strain Xen43) or no bacteria (uninfected) (see above) was subsequently placed into the pocket, and the surgical site was closed using Vicryl 5-0 sutures. For analgesia, sustained-release buprenorphine (ZooPharm) (2.5 mg/kg of body weight) was administered subcutaneously at the time of surgery.

Quantification of *in vivo S. epidermidis* burden (*in vivo* bioluminescence imaging). Mice were anesthetized with inhalation isoflurane (2%), and *in vivo* bioluminescence imaging was performed using a Lumina II imaging system (PerkinElmer, Inc.) as previously described (34, 35). Data are presented on a color scale overlaid on a grayscale photograph of mice and quantified as total flux (photons/s) within a circular region of interest (1×10^3 pixels) using Living Image software (PerkinElmer). For these experiments, the sample size was at least 8 mice per group and mice were imaged on days 0, 1, 3, 5, and 7.

Quantification of bacteria from the capsules and implants. Mice were euthanized on day 7, and the surgical implants with the surrounding tissue capsules were harvested. The capsules were separated from the implants, and bacteria in the capsules were isolated after the tissue was homogenized (Pro200 Series homogenizer; Pro Scientific, Oxford, CT). Bacteria adherent to the implants were detached by sonication in 1 ml 0.3% Tween 80–TSB for 10 min followed by vortex mixing for 5 min as previously described (34, 35). The number of bacterial CFU obtained from the capsules and implants was determined by counting CFU after overnight culture of plates. For these experiments, the sample size was at least 8 mice per group and CFU from the implants and joint tissue were harvested and counted on day 7.

Visualization of biofilms (VP-SEM). Mice were euthanized on day 7, and the titanium discs were harvested, the surrounding fibrous-tissue capsules were removed, and the surfaces of the implants were visualized using a field emission variable-pressure scanning electron microscope (VP-SEM) (FE-SEM Zeiss Supra VP40) as previously described (24, 34, 35). Pressure in the microscope chamber was maintained at 25 Pa to permit examination of the biofilms on the implant surface without the typical artifacts (dehydration, collapse, distortion, shrinkage, condensation, and aggregation) associated with conventional SEMs that require fixation and sputter coating (24, 35, 36). Thus, VP-SEM enabled the visualization of biofilms on the implants in their natural state. The sample size was 3 mice per group, and the VP-SEM imaging of the implant surface was performed on day 7.

Quantification of neutrophil recruitment (*in vivo* fluorescence imaging). The degree of inflammation in the postoperative site was measured by quantifying neutrophil infiltration, a correlate for inflammation and infection. This was accomplished by using LysEGFP mice, a genetically engineered mouse strain that possesses green-fluorescent neutrophils (24–26). LysEGFP mice were anesthetized with inhalation isoflurane (2%), and *in vivo* fluorescence imaging was performed using a Lumina II imaging system (PerkinElmer, Inc.) as previously described (35). Briefly, EGFP-expressing neutrophils at the postoperative site were visualized using the GFP filter for excitation (445 to 490 nm) and emission (515 to 575 nm) at an exposure time of 0.5 s. Data were quantified as total radiant efficiency ([photons/s]/[μW/cm^2]) within a circular region of interest (1×10^3 pixels) using Living Image software (PerkinElmer, Inc.). For these experiments, the sample size was at least 5 mice per group and mice were imaged on days 0, 1, 3, 5, 7, and 14.

Antibiotic therapy. The antibiotic doses were chosen to include a low dose (suboptimal) and high dose (effective) of cefazolin and vancomycin, and the low doses were combined with rifampin to evaluate the efficacy of combinatory prophylactic therapy. For cefazolin, our preliminary exper-

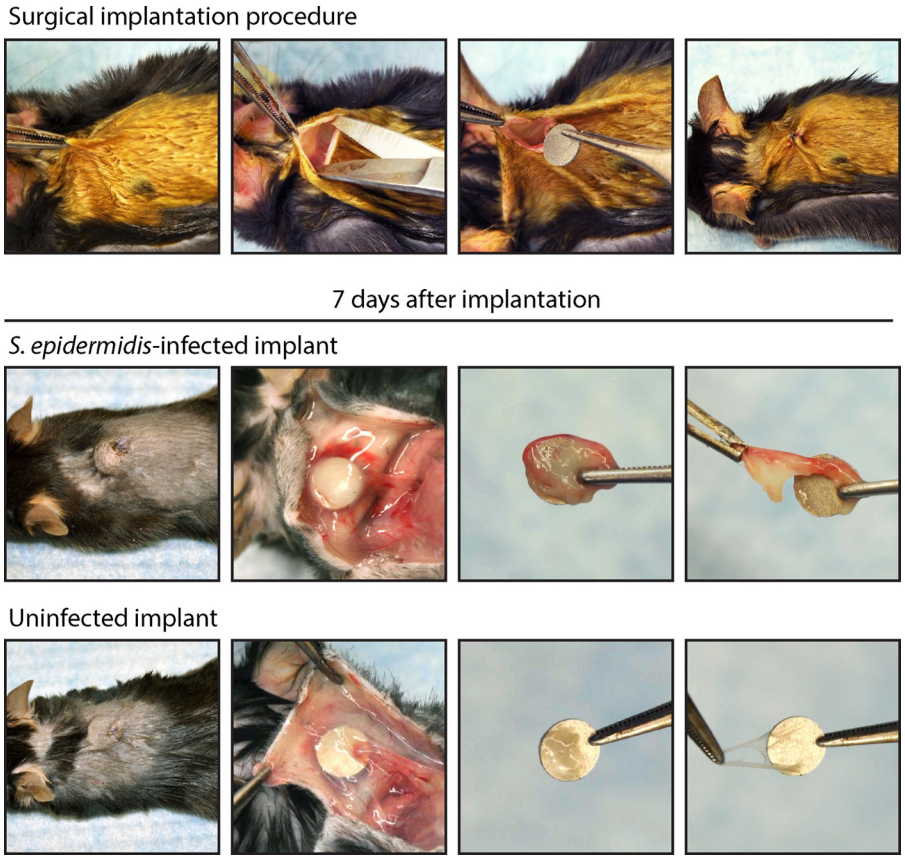

FIG 1 Mouse model of a subcutaneous-implant-related infection. Representative photographs of the surgical procedure are shown in the upper panels. A small skin incision was made on the upper dorsal backs of mice, and undermining was performed to create a subcutaneous pocket. A medical-procedure-grade titanium disc (5 mm in diameter and 0.4 mm thick) that had previously been incubated with *S. epidermidis* (infected) or no bacteria (uninfected) was subsequently placed into the pocket, and the surgical site was sutured closed. Representative photographs of the surgical site and harvesting of the surrounding tissue capsules and implants on postoperative day 7 are shown in the lower panels. The sizes and thicknesses of capsules were much more substantial in the infected implants than in the uninfected implants.

iments found that the 50 mg/kg dose (37, 38), which approximated the area under the concentration-time curve (AUC) of 670 mg · h/ml for the typical human exposure of cefazolin (2 g) (39), had a suboptimal effect in treating the *S. epidermidis* implant infection and was thus used as the low dose. For the high dose, 200 mg/kg of cefazolin was used, as doses above 50 mg/kg have increased efficacy against *S. aureus* skin infections in mice (37). For vancomycin, the low dose of 10 mg/kg was used, which approximated the 50% effective dose (ED_{50}) (10.6 mg/kg) in the neutropenic mouse thigh *S. aureus* infection model (40). For the high dose, 110 mg/kg of vancomycin was used (41), which approximated the AUC of 440 mg · h/ml for typical human exposure for vancomycin (1 g) (42, 43). For rifampin, the dose of 25 mg/kg was used based on previous studies that have used doses ranging from 20 to 25 mg/kg in various mouse models of staphylococcal infection in mice (44–48). There are important factors that influence matching the mouse doses to typical human exposures for cefazolin, vancomycin, and especially rifampin, including differences of half-life and serum protein binding between the species, and these are described in detail in the Discussion. Prophylactic therapy with vancomycin or cefazolin (both from Hospira, Inc., Lake Forest, IL) or a sham injection (saline solution) was administered intravenously via the retro-orbital vein 30 min preoperatively. To evaluate the efficacy of combination therapy, rifampin (25 mg/kg administered subcutaneously) (Pfizer, Inc., New York, NY) was added to the low-dose cefazolin or vancomycin prophylactic therapy. The *S. epidermidis* strain (Xen43) in this study had the following MICs: cefazolin ≤ 0.5 μg/ml, vancomycin ≤ 2 μg/ml, and rifampin ≤ 0.5 μg/ml. For these experiments, the sample size was 5 to 10 mice per group (all groups initially had an $n = 5$, and a second iteration was performed to confirm results for certain groups) and the efficacies of the prophylactic antibiotics were determined using *in vivo* bioluminescence imaging and *ex vivo* CFU counting (see above).

Statistical analysis. Data were compared using Student's *t* test (two tailed). All data are expressed as mean ± standard error of the mean. Values of $P < 0.05$ were considered statistically significant.

RESULTS

Mouse model of an implant-related infection. Using our *in vivo* model of a subcutaneous *S. epidermidis* implant infection (Fig. 1), we found that the bacterial bioluminescent signals of the 1×10^6, 1×10^7, and 1×10^8 CFU inocula differed on day 0 (2.5×10^6, 2.0×10^5, and 7.3×10^4 photons/s, respectively), became similar on day 1 (~2.5×10^5 photons/s), and then decreased to background levels (2×10^4 photons/s) by day 7 (Fig. 2A and B). The decreasing bioluminescent signals were likely a result of lower numbers of bacteria present as well as lower metabolic activity of bacteria as they began to form biofilms as previously described with this strain (23). Next, the CFU harvested from the capsules and implants were enumerated. Of note, *S. epidermidis*-infected mice formed larger fibrous-tissue capsules surrounding the im-

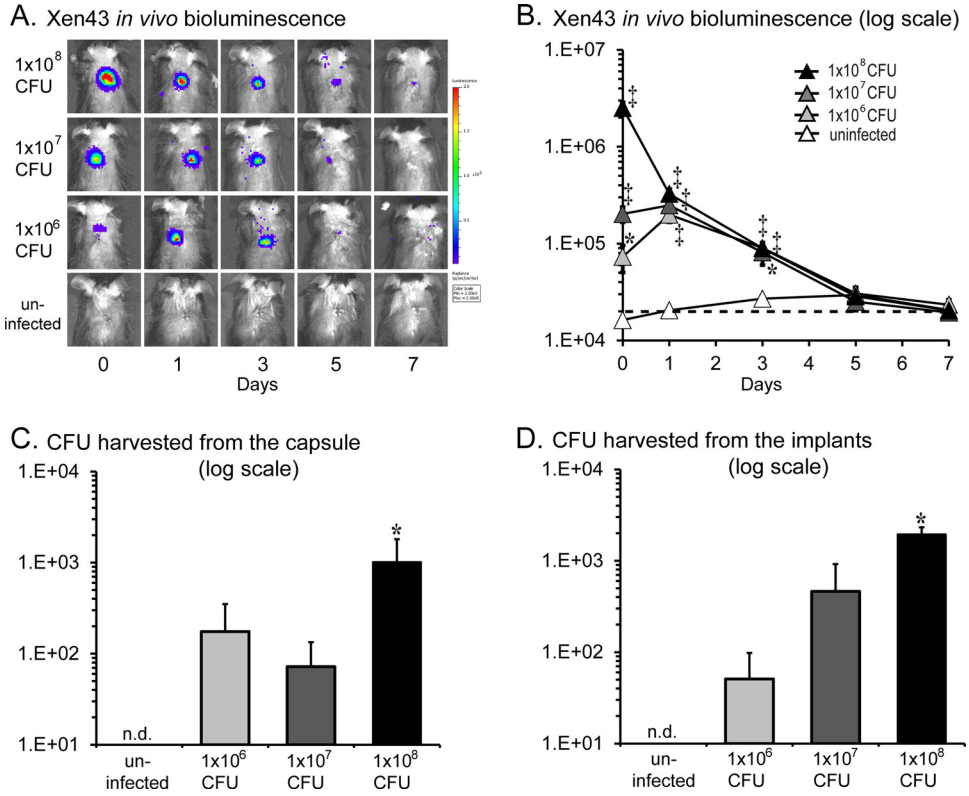

FIG 2 *In vivo S. epidermidis* bacterial burden. A medical-procedure-grade titanium disc incubated with a bioluminescent *S. epidermidis* strain (1×10^6, 1×10^7, or 1×10^8 CFU) or without bacteria (uninfected) was surgically placed into a subcutaneous pocket on the backs of mice to model an implant-related infection ($n = 8$ per group). (A) Representative *in vivo* bacterial bioluminescent signals on a color scale overlaid on a grayscale image of mice during the implant infection. (B) Quantification of *in vivo* bacterial bioluminescent signals (mean total flux [photons/s] ± standard error of the mean) (logarithmic scale). The dotted line denotes the level of background bioluminescence. (C and D) On postoperative day 7, the fibrous-tissue capsules and implants were harvested and the numbers of bacteria (mean CFU ± standard error of the mean) (logarithmic scale) isolated from the capsules (C) and implants (D) were determined. *, $P < 0.05$; †, $P < 0.01$; ‡, $P < 0.001$ (*S. epidermidis*-infected versus uninfected mice; Student's *t* test [two tailed]). n.d. = none detected.

plants than uninfected mice (Fig. 1, bottom panels). The CFU harvested from the capsules for the 1×10^6, 1×10^7, and 1×10^8 CFU inocula were 1.8×10^2, 7.2×10^2, and 1.0×10^3 CFU, respectively (Fig. 2C and D). Similarly, the CFU harvested from the discs for the 1×10^6, 1×10^7, and 1×10^8 CFU inocula were 5.1×10^1, 4.6×10^2, and 1.9×10^3 CFU, respectively. Since the inoculum of 1×10^8 CFU resulted in a consistent implant infection with the highest bioluminescent signals and numbers of CFU harvested from the capsules and implants, this inoculum was used in all subsequent experiments.

Biofilm formation. Biofilm formation was readily visualized from discs harvested from *S. epidermidis*-infected mice by the use of VP-SEM (Fig. 3). In contrast, uninfected mice, which did not have any bacterial inoculation, had no detectable biofilm formation as the VP-SEM images resembled the metal surface seen on the titanium discs prior to implantation. These data demonstrating the presence of biofilms on infected implants are consistent with the presence of CFU harvested from the surface of the implants in Fig. 2D as well as the biofilms that occur in CIED infections in patients (5, 6).

Simultaneous measurement of bacterial burden and neutrophil infiltration. To determine whether the presence of the *S. epidermidis* infection impacted the degree of neutrophil recruitment, our *in vivo* localized subcutaneous implant-related infection was performed in LysEGFP mice to simultaneously and noninvasively measure both bacterial burden and neutrophil infiltration using *in vivo* bioluminescent and fluorescent imaging, respectively (Fig. 4). Similarly to the C57BL/6 mice shown in Fig. 2, the *S. epidermidis*-infected LysEGFP mice developed bioluminescence signals that decreased over the course of the experiment until day 7, from which time they remained at the level of background bioluminescent signals through day 14. Interestingly, the *S. epidermidis*-infected LysEGFP mice had the same level of EGFP-neutrophil fluorescent signals as uninfected control mice on all postoperative days. The levels of EGFP-neutrophil fluorescent signals peaked on day 3 in both *S. epidermidis*-infected mice (6.7×10^9 [photons/s]/[μW/cm^2]) and uninfected mice (8.9×10^9 [photons/s]/[μW/cm^2]), and the signals decreased to background levels (1.8×10^9 [photons/s]/[μW/cm^2]) by postoperative day 14, when the experiment was arbitrarily terminated. Thus, despite the presence of a *S. epidermidis* infection, the EGFP-neutrophil fluorescent signals were not significantly different from those seen with the uninfected mice, suggesting that the low virulence of *S. epidermidis* did not increase the local inflammatory response compared with the level seen with the surgical procedure alone. Alternatively, the inflammation caused by the infection may have been a magnitude lower than that produced by the surgical procedure alone.

Efficacy of prophylactic antibiotics and impact on *in vivo* bioluminescence signals. This subcutaneous implant-related in-

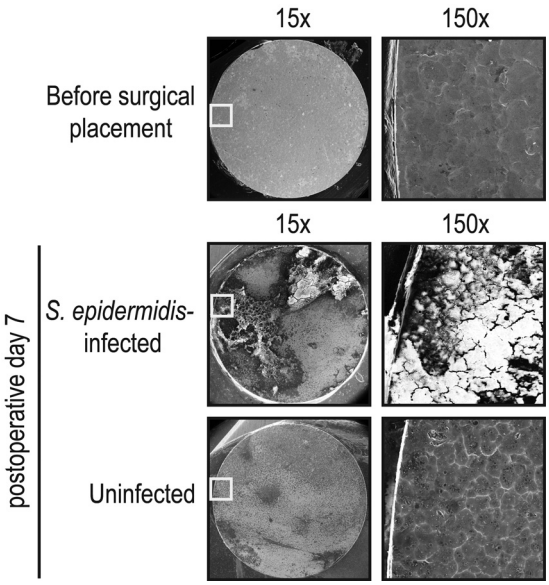

FIG 3 Biofilm formation on the implants. On postoperative day 7, the implants from *S. epidermidis*-infected and uninfected mice were harvested, the fibrous-tissue capsules were removed, and the surfaces of the titanium discs were analyzed for biofilm formation by variable-pressure scanning electron microscopy (VP-SEM). Representative VP-SEM images (representing 1 of 3 mice per group with similar results) are shown. The left panels represent a low-power magnification (×15), and the right panels show a higher magnification (×150) of the area boxed in white. Biofilm formation is readily seen on discs harvested from *S. epidermidis*-infected mice, whereas only the metal surface is seen on implants from uninfected mice.

fection model was used to evaluate the efficacies of low versus high doses of cefazolin (50 versus 200 mg/kg) or vancomycin (10 versus 110 mg/kg) with or without rifampin (25 mg/kg) in combination therapy. Sham control mice for the cefazolin experiments that were administered sterile saline solution had bioluminescence signals of $1.1 \times 10^6 \pm 2.1 \times 10^5$ photons/s, $2.2 \times 10^5 \pm 3.5 \times 10^4$ photons/s, and $1.3 \times 10^5 \pm 2.5 \times 10^4$ photons/s on days 0, 1, and 3, respectively, which subsequently decreased to background levels ($\sim 2 \times 10^4$ photons/s) by postoperative day 7 as previously observed (Fig. 2A and B). High-dose cefazolin resulted in 27.8-fold ($4.0 \times 10^4 \pm 1.2 \times 10^4$ photons/s), 7.1-fold ($3.0 \times 10^4 \pm 1.4 \times 10^4$ photons/s), and 3.5-fold ($3.7 \times 10^4 \pm 1.3 \times 10^4$ photons/s) reductions in bioluminescent signals on days 0, 1, and 3, respectively ($P < 0.01$). In contrast, low-dose cefazolin had a moderate level of efficacy and resulted in 8.8-fold ($1.3 \times 10^5 \pm 5.9 \times 10^4$ photons/s) and 4.2-fold ($5.2 \times 10^4 \pm 1.5 \times 10^4$ photons/s) statistically significant reductions in bioluminescent signals on postoperative days 0 and 1 ($P < 0.05$), after which the signals did not significantly differ from those seen with sham-treated mice. The addition of rifampin to the low-dose cefazolin resulted in a modest further reduction in bioluminescent signals (3.5-fold [$3.1 \times 10^4 \pm 2.1 \times 10^3$ photons/s] on day 1 compared with cefazolin alone [$P < 0.05$]). However, after day 1, the bioluminescent signals of the cefazolin-rifampin combination no longer differed from those seen with the low-dose cefazolin treatment alone.

Similarly to the sham-treated mice for the cefazolin experiments, sham control mice for the vancomycin experiments had bioluminescence signals of $1.1 \times 10^6 \pm 2.3 \times 10^5$ photons/s, $2.3 \times 10^5 \pm 3.9 \times 10^4$ photons/s, $1.2 \times 10^5 \pm 2.6 \times 10^4$ photons/s, and $3.6 \times 10^4 \pm 5.0 \times 10^3$ photons/s on days 0, 1, 3, and 5, respectively, which subsequently decreased to background levels ($\sim 2 \times 10^4$ photons/s) by postoperative day 7. High-dose vancomycin resulted in 44-fold ($2.4 \times 10^4 \pm 3.2 \times 10^3$ photons/s), 9-fold ($2.5 \times 10^4 \pm 2.4 \times 10^3$ photons/s), and 3-fold ($3.9 \times 10^4 \pm 1.0 \times 10^4$ photons/s) reductions on days 0, 1, and 3, respectively ($P < 0.01$). In contrast, low-dose vancomycin lacked any therapeutic effect as the bioluminescent signals did not differ from those seen with the sham treatment. In contrast, the vancomycin (low dose)-rifampin combination had a marked therapeutic effect, with 40-fold ($2.6 \times 10^4 \pm 3.4 \times 10^3$ photons/s), 10.6-fold ($2.6 \times 10^4 \pm 6.5 \times 10^2$ photons/s), 2.4-fold ($2.8 \times 10^4 \pm 1.8 \times 10^3$ photons/s), and 1.2-fold ($2.9 \times 10^4 \pm 1.3 \times 10^3$ photons/s) statistically significant reductions in bioluminescent signals on postoperative days 0, 1, 3, and 5, respectively ($P < 0.05$) compared with low-dose vancomycin treatment alone.

In summary, high-dose cefazolin and high-dose vancomycin resulted in similarly decreased bioluminescence signals whereas low-dose cefazolin but not low-dose vancomycin prophylaxis resulted in decreased bioluminescent signals compared with sham treatment. Furthermore, the addition of rifampin to low-dose vancomycin but not to low-dose cefazolin led to a marked decrease in bioluminescent signals.

Effect of the prophylactic antibiotics on *ex vivo* bacterial counts. To confirm the findings obtained with *in vivo* bioluminescence imaging (Fig. 5A), *ex vivo* CFU were enumerated from the capsules and implants (Fig. 5B and C). Sham control mice averaged $6.0 \times 10^2 \pm 2.2 \times 10^2$ CFU harvested from the capsules and $1.5 \times 10^3 \pm 2.1 \times 10^2$ CFU isolated from the implants. High-dose cefazolin prophylaxis and high-dose vancomycin prophylaxis were both highly efficacious, as either prophylactic antibiotic therapy resulted in virtually no CFU harvested from the capsules (cefazolin = no CFU isolated and vancomycin = $1.0 \times 10^0 \pm 1.0 \times 10^0$ CFU) or the implants (cefazolin = $1.5 \times 10^0 \pm 1.5 \times 10^0$ CFU and vancomycin = no CFU isolated) ($P < 0.05$). In contrast, low-dose cefazolin and vancomycin were moderately efficacious, as they resulted in statistically significant decreased CFU harvested from the capsules (14.9-fold [$4.1 \times 10^1 \pm 2.3 \times 10^1$ CFU] and 9.9-fold [$7.3 \times 10^1 \pm 9.8 \times 10^1$ CFU], respectively) and implants (143-fold [$1.0 \times 10^1 \pm 9.4 \times 10^0$ CFU] and 86-fold [$2.1 \times 10^1 \pm 1.4 \times 10^1$ CFU], respectively) compared with sham treatment ($P < 0.05$). Interestingly, the addition of rifampin to low-dose cefazolin did not result in a further reduction of CFU harvested from the capsules compared to low-dose cefazolin alone but resulted in no CFU harvested from the implants. In contrast, the addition of rifampin to the low-dose vancomycin resulted in a substantial reduction of CFU as there were virtually no CFU harvested from either the capsules ($1.0 \times 10^0 \pm 1.0 \times 10^0$ CFU) or the implants (no CFU isolated).

DISCUSSION

Infections associated with CIED are difficult to diagnose and treat and may lead to life-threatening complications (2–4). Since improved antibiotic prophylaxis may further reduce the rate of infections, we developed a preclinical mouse model of a *S. epidermidis* localized subcutaneous implant infection to evaluate the efficacy of antibiotic prophylaxis. We found that high therapeutic doses of cefazolin or vancomycin were effective in reducing *in vivo* bacterial bioluminescent signals and *ex vivo* CFU from the sur-

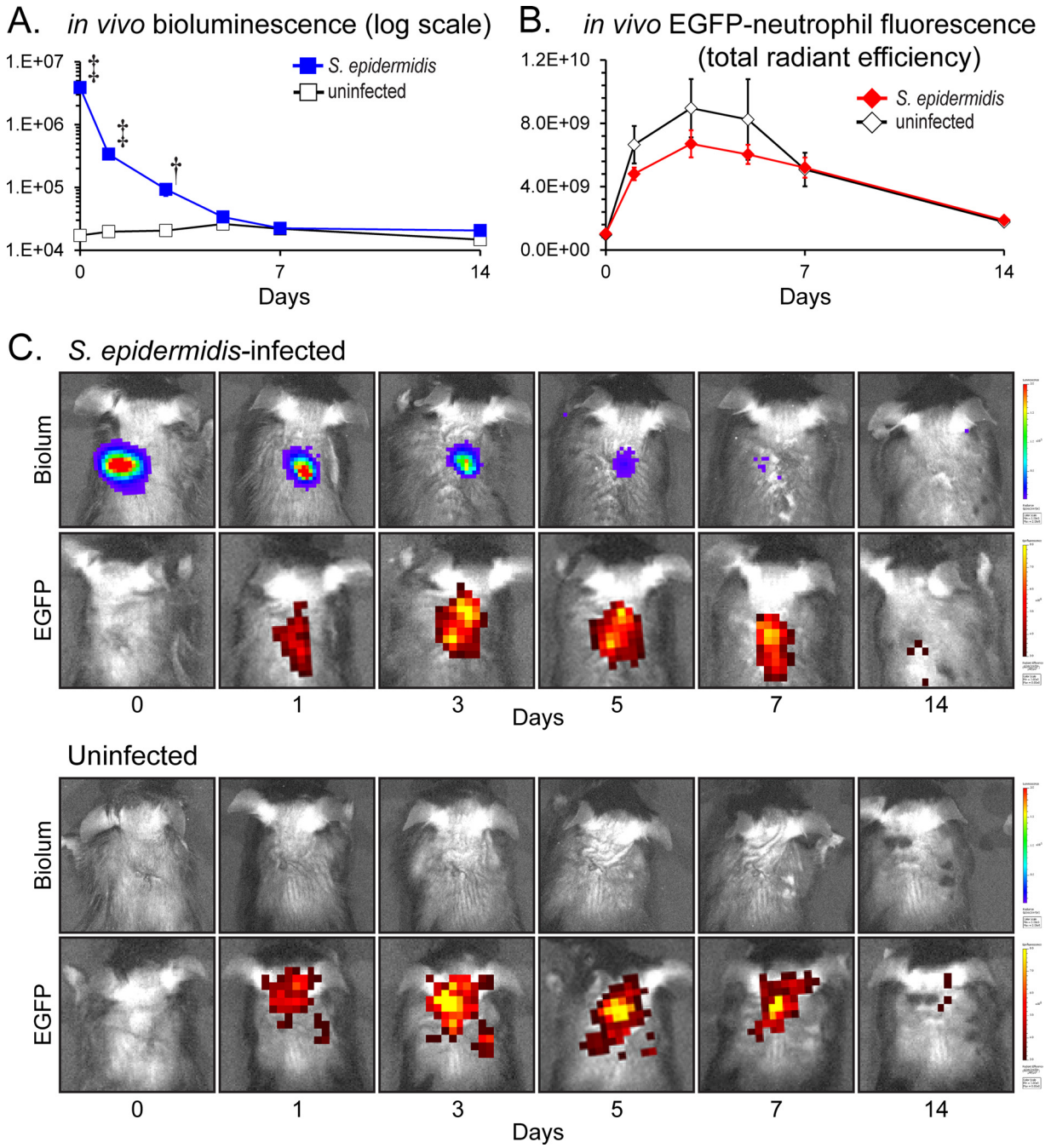

FIG 4 Measurement of bacterial burden and neutrophil infiltration using *in vivo* bioluminescence and fluorescence imaging. A medical-procedure-grade titanium disc incubated with a bioluminescent *S. epidermidis* strain (1×10^8 CFU) or without bacteria (uninfected) was surgically placed into a subcutaneous pocket on the backs of mice to model an implant-related infection ($n = 8$ per group). (A) Mean bacterial burden as measured by *in vivo* bioluminescence imaging (mean total flux [photons/s] ± standard errors of the means) (logarithmic scale). (B) Mean neutrophil infiltration as measured by *in vivo* fluorescence imaging (mean total radiant efficiency [photons/s]/[μW/cm^2] ± standard error of the mean). *, $P < 0.05$; †, $P < 0.01$; ‡, $P < 0.001$ (*S. epidermidis*-infected mice versus uninfected mice; Student's *t* test [two tailed]). (C) Representative images of *in vivo* bioluminescent signals (Biolum; upper panels) and *in vivo* fluorescent signals (EGFP; lower panels) on a color scale overlaid on grayscale images of a *S. epidermidis*-infected mouse and an uninfected mouse.

rounding tissue capsules and the implants. In contrast, suboptimal low doses of cefazolin or vancomycin reduced the *in vivo* bioluminescent signals and *ex vivo* CFU only moderately. The addition of rifampin to low-dose vancomycin was highly effective in reducing *in vivo* and *ex vivo* bacterial burden. Interestingly, the addition of rifampin to low-dose cefazolin was less effective, since CFU were reduced from the implants but not the capsules. Taken together, these results suggest that rifampin combination therapy had a therapeutic benefit as a prophylactic therapy when combined with vancomycin and to a lesser extent with cefazolin.

There are several factors that should be taken into account when interpreting the *in vivo* bioluminescence data. First, al-

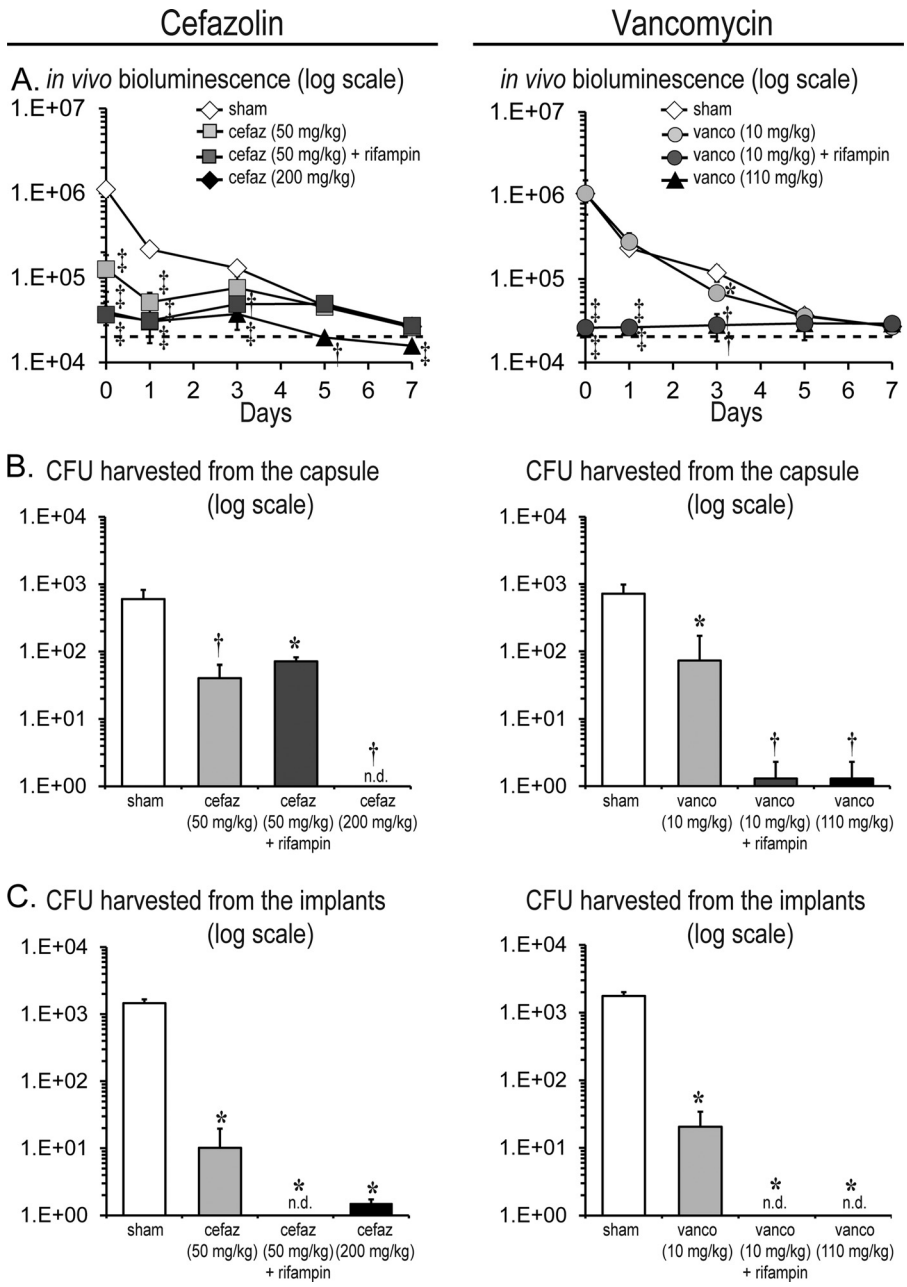

FIG 5 Efficacy of prophylactic antibiotic therapy. A medical-procedure-grade titanium disc incubated with a bioluminescent *S. epidermidis* strain (1×10^8 CFU) was surgically placed into a subcutaneous pocket on the backs of mice to model an implant-related infection ($n = 5$ to 10 per group). The following prophylactic antibiotic treatment or sham treatment with sterile saline solution (sham) was administered to the mice 30 min preoperatively: cefazolin (cefaz; 50 mg/kg of body weight) ± rifampin (25 mg/kg) or cefazolin (200 mg/kg) (left panels) or vancomycin (vanco; 10 mg/kg) ± rifampin (25 mg/kg) or vancomycin (110 mg/kg) (right panels). (A) Bacterial burden as measured by *in vivo* bioluminescence (mean total flux [photons/s] ± standard error of the mean) (logarithmic scale). The dotted line denotes the level of background bioluminescence. (B and C) On postoperative day 7, the capsules and titanium discs were harvested and the numbers of bacteria (mean CFU ± standard error of the mean [logarithmic scale]) isolated from the capsules (B) and implants (C) were determined. *, $P < 0.05$; †, $P < 0.01$; ‡, $P < 0.001$ (prophylactic antibiotic-treated mice versus sham treatment; Student's *t* test [two tailed]). n.d. = none detected.

though Xen43 has a stable *lux* construct integrated into the bacterial chromosome (23), the bioluminescent signals decreased to background levels by day 7 despite the presence of CFU in the capsules and on the implants. The reason for this is likely due to the low metabolic activity of bacteria as they form biofilms as we previously observed with Xen43 in a subcutaneous catheter biofilm infection mouse model (23). Second, an inoculum of 1×10^8 CFU *S. epidermidis* (which was similar to the 5×10^7 CFU inoculum in the subcutaneous catheter model [23]) was required to produce an implant infection with consistent *ex vivo* CFU isolated from the capsules and implants (Fig. 2C and D). In contrast, lower inocula resulted in more-variable numbers of *ex vivo* CFU, which did not reach statistical significance. The relatively high inoculum of 1×10^8 CFU required to induce an implant infection in this

model is likely due to the low virulence of *S. epidermidis* and the subcutaneous site of infection, which induced robust postoperative neutrophil recruitment in LysEGFP mice that was the same in the presence of the *S. epidermidis* infection and the surgical procedure alone (Fig. 4).

There are also important factors pertaining to the approximation of the human exposures of cefazolin, vancomycin, and rifampin in mice that should be taken into account in comparing exposures between the species. First, there are differences in serum protein binding, and the amount of drug bound is higher in humans versus mice for cefazolin (~85% versus ~50% [49–51]), vancomycin (35% to 50% versus ~25% [52, 53]), and rifampin (~97% versus ~90% [54]). Thus, the amount of free and active drug for these antibiotics is higher in mice than in humans. Second, the half-lives are much longer in humans versus mice for cefazolin (2 h versus 30 min [55, 56]) and vancomycin (7.7 h versus 2 h [42, 57]). Since the infected discs were implanted 30 min after administering the prophylactic antibiotics, the increased half-life of vancomycin may have contributed to its showing better effectiveness than cefazolin. Conversely, the half-life of rifampin is 4 h in humans and 12 h in mice (58, 59), indicating that rifampin has a prolonged effect in mice and providing an explanation for the increased efficacy of rifampin in this study. It should be mentioned that the typical human exposure of rifampin (10 mg/kg or 600 mg daily) was originally based on a combination of pharmacokinetics, toxicity, and cost (45, 60). At this dose, the AUC values are 48.5 μg · h/ml in humans and 132 μg · h/ml in mice (54). However, as mentioned above, the amount unbound drug is 3-fold higher and the half-life is 3-fold shorter in humans than in mice, making it difficult to match the human exposure. Taken together, these differences in the pharmacokinetics and pharmacodynamics (PK/PD) of the antibiotics between the species highlight the limitations of approximating human exposures in mice. Ideally, for evaluating a range of antibiotic doses, additional clinical *S. epidermidis* isolates as well as other bacterial strains that cause CIED infections (with various antibiotic susceptibilities) would provide more-precise PK/PD data to better match the exposures in humans and provide greater evidence of efficacy. These studies are to be the subject of our future investigations.

From a mechanistic standpoint, although the precise reason for the increased efficacy of rifampin combination therapy in our model is unknown, previous studies have found that rifampin has enhanced activity against bacteria in biofilms (27–30). This antibiofilm activity is consistent with our findings since cefazolin-rifampin- and vancomycin-rifampin-treated mice had no CFU isolated from the implants. In addition, a prior study found that bacteria in biofilms have increased cell wall thickness, rendering them less sensitive to vancomycin (61). Since both vancomycin and cefazolin act by disrupting bacterial cell wall synthesis, these antibiotics may be less active against bacteria in biofilms. In contrast, rifampin acts by inhibiting bacterial DNA-dependent RNA synthesis by binding to the bacterial RNA polymerase (62, 63).

From a clinical perspective, there are several factors that are important to take into account in considering rifampin combination as prophylactic therapy. Rifampin can cause toxicity, including hepatitis and drug interactions (32). In addition, although early reports found that rifampin combination prophylactic therapy had a therapeutic benefit in patients prior to cardiac valve replacement and cardiac bypass surgery (64, 65), these patients developed rifampin-resistant *S. epidermidis* infections in their normal human skin flora (66). However, certain combinations, such as daptomycin and rifampin, have been shown to decrease the development of resistance in an experimental vascular graft biofilm model (67).

Taken together, our findings suggest that antibiotic prophylaxis against CIED and perhaps other surgical implant infections can be further optimized to prevent infectious complications and improve clinical outcomes. In particular, a reexamination and reconsideration of rifampin combination as prophylactic therapy may be warranted in certain patient populations at highest risk for CIED infections as these infections can have deadly consequences. Alternatively, other antistaphylococcal drugs with longer half-lives such as tetracyclines (doxycycline, minocycline, or tigecycline) or newer glycopeptides (daptomycin, telavancin, dalbavancin, or oritavancin) could serve as additional candidates for combination prophylactic therapy and our mouse model could serve as a valuable preclinical system to evaluate these potential antibiotic combinations before initiating clinical trials.

ACKNOWLEDGMENTS

This work was supported by the Medtronic, Inc., CRDM (Cardiac Rhythm Disease Management) External Research Program (to D.Z.U. and L.S.M.), an H & H Lee Surgical Resident Research Scholars Program (to A.I.S. and J.A.N.), the Intramural Program of the National Institute of Allergy and Infectious Diseases (NIAID), the National Institutes of Health (to M. O.), and National Institutes of Health grants R24-CA92865 (to the UCLA Small Animal Imaging Resource Program), R01 HS021188 (to D.Z.U.), and R01-AI078910 (to L.S.M.).

REFERENCES

1. **Darouiche RO.** 2004. Treatment of infections associated with surgical implants. N. Engl. J. Med. **350:**1422–1429. http://dx.doi.org/10.1056/NEJMra035415.
2. **Uslan DZ, Baddour LM.** 2006. Cardiac device infections: getting to the heart of the matter. Curr. Opin. Infect. Dis. **19:**345–348. http://dx.doi.org/10.1097/01.qco.0000235160.78302.24.
3. **Gould PA, Gula LJ, Yee R, Skanes AC, Klein GJ, Krahn AD.** 2011. Cardiovascular implantable electrophysiological device-related infections: a review. Curr. Opin. Cardiol. **26:**6–11. http://dx.doi.org/10.1097/HCO.0b013e328341384e.
4. **Baddour LM, Epstein AE, Erickson CC, Knight BP, Levison ME, Lockhart PB, Masoudi FA, Okum EJ, Wilson WR, Beerman LB, Bolger AF, Estes NA, III, Gewitz M, Newburger JW, Schron EB, Taubert KA, American Heart Association Rheumatic Fever, Endocarditis, and Kawasaki Disease Committee; Council on Cardiovascular Disease in Young; Council on Cardiovascular Surgery and Anesthesia; Council on Cardiovascular Nursing; Council on Clinical Cardiology; Interdisciplinary Council on Quality of Care; American Heart Association.** 2010. Update on cardiovascular implantable electronic device infections and their management: a scientific statement from the American Heart Association. Circulation **121:**458–477. http://dx.doi.org/10.1161/CIRCULATIONAHA.109.192665.
5. **Toba FA, Akashi H, Arrecubieta C, Lowy FD.** 2011. Role of biofilm in Staphylococcus aureus and Staphylococcus epidermidis ventricular assist device driveline infections. J. Thorac. Cardiovasc. Surg. **141:**1259–1264. http://dx.doi.org/10.1016/j.jtcvs.2010.07.016.
6. **Rohacek M, Weisser M, Kobza R, Schoenenberger AW, Pfyffer GE, Frei R, Erne P, Trampuz A.** 2010. Bacterial colonization and infection of electrophysiological cardiac devices detected with sonication and swab culture. Circulation **121:**1691–1697. http://dx.doi.org/10.1161/CIRCULATIONAHA.109.906461.
7. **Kolker AR, Redstone JS, Tutela JP.** 2007. Salvage of exposed implantable cardiac electrical devices and lead systems with pocket change and local flap coverage. Ann. Plast. Surg. **59:**26–29. http://dx.doi.org/10.1097/01.sap.0000261846.73531.2e.
8. **Sohail MR, Uslan DZ, Khan AH, Friedman PA, Hayes DL, Wilson WR, Steckelberg JM, Stoner S, Baddour LM.** 2007. Management and outcome of permanent pacemaker and implantable cardioverter-defibrillator in-

fections. J. Am. Coll. Cardiol. **49:**1851–1859. http://dx.doi.org/10.1016/j.jacc.2007.01.072.
9. **Tascini C, Bongiorni MG, Gemignani G, Soldati E, Leonildi A, Arena G, Doria R, Giannola G, La Pira F, Tagliaferri E, Caravelli P, Dell'Anna R, Menichetti F.** 2006. Management of cardiac device infections: a retrospective survey of a non-surgical approach combining antibiotic therapy with transvenous removal. J. Chemother. **18:**157–163. http://dx.doi.org/10.1179/joc.2006.18.2.157.
10. **Bloom HL, Constantin L, Dan D, De Lurgio DB, El-Chami M, Ganz LI, Gleed KJ, Hackett FK, Kanuru NK, Lerner DJ, Rasekh A, Simons GR, Sogade FO, Sohail MR; COoperative Multicenter study Monitoring a CIED ANtimicrobial Device Investigators.** 2011. Implantation success and infection in cardiovascular implantable electronic device procedures utilizing an antibacterial envelope. Pacing Clin. Electrophysiol. **34:**133–142. http://dx.doi.org/10.1111/j.1540-8159.2010.02931.x.
11. **Sohail MR, Uslan DZ, Khan AH, Friedman PA, Hayes DL, Wilson WR, Steckelberg JM, Stoner SM, Baddour LM.** 2007. Risk factor analysis of permanent pacemaker infection. Clin. Infect. Dis. **45:**166–173. http://dx.doi.org/10.1086/518889.
12. **de Oliveira JC, Martinelli M, Nishioka SA, Varejao T, Uipe D, Pedrosa AA, Costa R, D'Avila A, Danik SB.** 2009. Efficacy of antibiotic prophylaxis before the implantation of pacemakers and cardioverter-defibrillators: results of a large, prospective, randomized, double-blinded, placebo-controlled trial. Circ. Arrhythm. Electrophysiol. **2:**29–34. http://dx.doi.org/10.1161/CIRCEP.108.795906.
13. **Da Costa A, Kirkorian G, Cucherat M, Delahaye F, Chevalier P, Cerisier A, Isaaz K, Touboul P.** 1998. Antibiotic prophylaxis for permanent pacemaker implantation: a meta-analysis. Circulation **97:**1796–1801. http://dx.doi.org/10.1161/01.CIR.97.18.1796.
14. **Uslan DZ, Gleva MJ, Warren DK, Mela T, Chung MK, Gottipaty V, Borge R, Dan D, Shinn T, Mitchell K, Holcomb RG, Poole JE.** 2012. Cardiovascular implantable electronic device replacement infections and prevention: results from the REPLACE Registry. Pacing Clin. Electrophysiol. **35:**81–87. http://dx.doi.org/10.1111/j.1540-8159.2011.03257.x.
15. **Darouiche R, Mosier M, Voigt J.** 2012. Antibiotics and antiseptics to prevent infection in cardiac rhythm management device implantation surgery. Pacing Clin. Electrophysiol. **35:**1348–1360. http://dx.doi.org/10.1111/j.1540-8159.2012.03506.x.
16. **Margey R, McCann H, Blake G, Keelan E, Galvin J, Lynch M, Mahon N, Sugrue D, O'Neill J.** 2010. Contemporary management of and outcomes from cardiac device related infections. Europace **12:**64–70. http://dx.doi.org/10.1093/europace/eup362.
17. **Anselmino M, Vinci M, Comoglio C, Rinaldi M, Bongiorni MG, Trevi GP, Golzio PG.** 2009. Bacteriology of infected extracted pacemaker and ICD leads. J. Cardiovasc. Med. (Hagerstown) **10:**693–698. http://dx.doi.org/10.2459/JCM.0b013e32832b3585.
18. **Uslan DZ, Sohail MR, St Sauver JL, Friedman PA, Hayes DL, Stoner SM, Wilson WR, Steckelberg JM, Baddour LM.** 2007. Permanent pacemaker and implantable cardioverter defibrillator infection: a population-based study. Arch. Intern. Med. **167:**669–675. http://dx.doi.org/10.1001/archinte.167.7.669.
19. **Dy Chua J, Abdul-Karim A, Mawhorter S, Procop GW, Tchou P, Niebauer M, Saliba W, Schweikert R, Wilkoff BL.** 2005. The role of swab and tissue culture in the diagnosis of implantable cardiac device infection. Pacing Clin. Electrophysiol. **28:**1276–1281. http://dx.doi.org/10.1111/j.1540-8159.2005.00268.x.
20. **Chambers ST.** 2005. Diagnosis and management of staphylococcal infections of pacemakers and cardiac defibrillators. Intern. Med. J. **35**(Suppl 2)**:**S63–S71. http://dx.doi.org/10.1111/j.1444-0903.2005.00980.x.
21. **Greenspon AJ, Patel JD, Lau E, Ochoa JA, Frisch DR, Ho RT, Pavri BB, Kurtz SM.** 2011. 16-Year trends in the infection burden for pacemakers and implantable cardioverter-defibrillators in the United States 1993 to 2008. J. Am. Coll. Cardiol. **58:**1001–1006. http://dx.doi.org/10.1016/j.jacc.2011.04.033.
22. **Voigt A, Shalaby A, Saba S.** 2010. Continued rise in rates of cardiovascular implantable electronic device infections in the United States: temporal trends and causative insights. Pacing Clin. Electrophysiol. **33:**414–419. http://dx.doi.org/10.1111/j.1540-8159.2009.02569.x.
23. **Vuong C, Kocianova S, Yu J, Kadurugamuwa JL, Otto M.** 2008. Development of real-time in vivo imaging of device-related Staphylococcus epidermidis infection in mice and influence of animal immune status on susceptibility to infection. J. Infect. Dis. **198:**258–261. http://dx.doi.org/10.1086/589307.
24. **Bernthal NM, Stavrakis AI, Billi F, Cho JS, Kremen TJ, Simon SI, Cheung AL, Finerman GA, Lieberman JR, Adams JS, Miller LS.** 2010. A mouse model of post-arthroplasty Staphylococcus aureus joint infection to evaluate in vivo the efficacy of antimicrobial implant coatings. PLoS One **5:**e12580. http://dx.doi.org/10.1371/journal.pone.0012580.
25. **Faust N, Varas F, Kelly LM, Heck S, Graf T.** 2000. Insertion of enhanced green fluorescent protein into the lysozyme gene creates mice with green fluorescent granulocytes and macrophages. Blood **96:**719–726.
26. **Niska JA, Meganck JA, Pribaz JR, Shahbazian JH, Lim E, Zhang N, Rice BW, Akin A, Ramos RI, Bernthal NM, Francis KP, Miller LS.** 2012. Monitoring bacterial burden, inflammation and bone damage longitudinally using optical and micro-CT imaging in an orthopaedic implant infection in mice. PLoS One **7:**e47397. http://dx.doi.org/10.1371/journal.pone.0047397.
27. **John AK, Baldoni D, Haschke M, Rentsch K, Schaerli P, Zimmerli W, Trampuz A.** 2009. Efficacy of daptomycin in implant-associated infection due to methicillin-resistant Staphylococcus aureus: importance of combination with rifampin. Antimicrob. Agents Chemother. **53:**2719–2724. http://dx.doi.org/10.1128/AAC.00047-09.
28. **Raad I, Hanna H, Jiang Y, Dvorak T, Reitzel R, Chaiban G, Sherertz R, Hachem R.** 2007. Comparative activities of daptomycin, linezolid, and tigecycline against catheter-related methicillin-resistant Staphylococcus bacteremic isolates embedded in biofilm. Antimicrob. Agents Chemother. **51:**1656–1660. http://dx.doi.org/10.1128/AAC.00350-06.
29. **Saginur R, Stdenis M, Ferris W, Aaron SD, Chan F, Lee C, Ramotar K.** 2006. Multiple combination bactericidal testing of staphylococcal biofilms from implant-associated infections. Antimicrob. Agents Chemother. **50:**55–61. http://dx.doi.org/10.1128/AAC.50.1.55-61.2006.
30. **Parra-Ruiz J, Vidaillac C, Rose WE, Rybak MJ.** 2010. Activities of high-dose daptomycin, vancomycin, and moxifloxacin alone or in combination with clarithromycin or rifampin in a novel in vitro model of Staphylococcus aureus biofilm. Antimicrob. Agents Chemother. **54:**4329–4334. http://dx.doi.org/10.1128/AAC.00455-10.
31. **Liu C, Bayer A, Cosgrove SE, Daum RS, Fridkin SK, Gorwitz RJ, Kaplan SL, Karchmer AW, Levine DP, Murray BE, Rybak J, Talan DA, Chambers HF.** 2011. Clinical practice guidelines by the Infectious Diseases Society of America for the treatment of methicillin-resistant Staphylococcus aureus infections in adults and children. Clin. Infect. Dis. **52:**e18–e55. http://dx.doi.org/10.1093/cid/ciq146.
32. **Osmon DR, Berbari EF, Berendt AR, Lew D, Zimmerli W, Steckelberg JM, Rao N, Hanssen A, Wilson WR.** 2013. Diagnosis and management of prosthetic joint infection: clinical practice guidelines by the Infectious Diseases Society of America. Clin. Infect. Dis. **56:**e1–e25. http://dx.doi.org/10.1093/cid/cis803.
33. **Mack D, Siemssen N, Laufs R.** 1992. Parallel induction by glucose of adherence and a polysaccharide antigen specific for plastic-adherent Staphylococcus epidermidis: evidence for functional relation to intercellular adhesion. Infect. Immun. **60:**2048–2057.
34. **Niska JA, Shahbazian JH, Ramos RI, Pribaz JR, Billi F, Francis KP, Miller LS.** 2012. Daptomycin and tigecycline have broader effective dose ranges than vancomycin as prophylaxis against a Staphylococcus aureus surgical implant infection in mice. Antimicrob. Agents Chemother. **56:**2590–2597. http://dx.doi.org/10.1128/AAC.06291-11.
35. **Pribaz JR, Bernthal NM, Billi F, Cho JS, Ramos RI, Guo Y, Cheung AL, Francis KP, Miller LS.** 2012. Mouse model of chronic post-arthroplasty infection: noninvasive in vivo bioluminescence imaging to monitor bacterial burden for long-term study. J. Orthop. Res. **30:**335–340. http://dx.doi.org/10.1002/jor.21519.
36. **Bernthal NM, Pribaz JR, Stavrakis AI, Billi F, Cho JS, Ramos RI, Francis KP, Iwakura Y, Miller LS.** 2011. Protective role of IL-1beta against post-arthroplasty Staphylococcus aureus infection. J. Orthop. Res. **29:**1621–1626. http://dx.doi.org/10.1002/jor.21414.
37. **Fernandez J, Hilliard JJ, Abbanat D, Zhang W, Melton JL, Santoro CM, Flamm RK, Bush K.** 2010. In vivo activity of ceftobiprole in murine skin infections due to Staphylococcus aureus and Pseudomonas aeruginosa. Antimicrob. Agents Chemother. **54:**116–125. http://dx.doi.org/10.1128/AAC.00642-09.
38. **Xiong YQ, Willard J, Kadurugamuwa JL, Yu J, Francis KP, Bayer AS.** 2005. Real-time in vivo bioluminescent imaging for evaluating the efficacy of antibiotics in a rat Staphylococcus aureus endocarditis model. Antimicrob. Agents Chemother. **49:**380–387. http://dx.doi.org/10.1128/AAC.49.1.380-387.2005.
39. **Douglas A, Udy AA, Wallis SC, Jarrett P, Stuart J, Lassig-Smith M,**

Deans R, Roberts MS, Taraporewalla K, Jenkins J, Medley G, Lipman J, Roberts JA. 2011. Plasma and tissue pharmacokinetics of cefazolin in patients undergoing elective and semielective abdominal aortic aneurysm open repair surgery. Antimicrob. Agents Chemother. **55:**5238–5242. http://dx.doi.org/10.1128/AAC.05033-11.

40. **Hegde SS, Reyes N, Wiens T, Vanasse N, Skinner R, McCullough J, Kaniga K, Pace J, Thomas R, Shaw JP, Obedencio G, Judice JK.** 2004. Pharmacodynamics of telavancin (TD-6424), a novel bactericidal agent, against gram-positive bacteria. Antimicrob. Agents Chemother. **48:**3043–3050. http://dx.doi.org/10.1128/AAC.48.8.3043-3050.2004.
41. **Reyes N, Skinner R, Kaniga K, Krause KM, Shelton J, Obedencio GP, Gough A, Conner M, Hegde SS.** 2005. Efficacy of telavancin (TD-6424), a rapidly bactericidal lipoglycopeptide with multiple mechanisms of action, in a murine model of pneumonia induced by methicillin-resistant Staphylococcus aureus. Antimicrob. Agents Chemother. **49:**4344–4346. http://dx.doi.org/10.1128/AAC.49.10.4344-4346.2005.
42. **Reyes N, Skinner R, Benton BM, Krause KM, Shelton J, Obedencio GP, Hegde SS.** 2006. Efficacy of telavancin in a murine model of bacteraemia induced by methicillin-resistant Staphylococcus aureus. J. Antimicrob. Chemother. **58:**462–465. http://dx.doi.org/10.1093/jac/dkl222.
43. **Crandon JL, Kuti JL, Nicolau DP.** 2010. Comparative efficacies of human simulated exposures of telavancin and vancomycin against methicillin-resistant Staphylococcus aureus with a range of vancomycin MICs in a murine pneumonia model. Antimicrob. Agents Chemother. **54:**5115–5119. http://dx.doi.org/10.1128/AAC.00062-10.
44. **Sakoulas G, Eliopoulos GM, Alder J, Eliopoulos CT.** 2003. Efficacy of daptomycin in experimental endocarditis due to methicillin-resistant Staphylococcus aureus. Antimicrob. Agents Chemother. **47:**1714–1718. http://dx.doi.org/10.1128/AAC.47.5.1714-1718.2003.
45. **van Ingen J, Aarnoutse RE, Donald PR, Diacon AH, Dawson R, Plemper van Balen G, Gillespie SH, Boeree MJ.** 2011. Why do we use 600 mg of rifampicin in tuberculosis treatment? Clin. Infect. Dis. **52:**e194–e199. http://dx.doi.org/10.1093/cid/cir184.
46. **Mandell GL, Moorman DR.** 1980. Treatment of experimental staphylococcal infections: effect of rifampin alone and in combination on development of rifampin resistance. Antimicrob. Agents Chemother. **17:**658–662. http://dx.doi.org/10.1128/AAC.17.4.658.
47. **Lobo MC, Mandell GL.** 1972. Treatment of experimental staphylococcal infection with rifampin. Antimicrob. Agents Chemother. **2:**195–200. http://dx.doi.org/10.1128/AAC.2.3.195.
48. **Mandell GL, Vest TK.** 1972. Killing of intraleukocytic Staphylococcus aureus by rifampin: in-vitro and in-vivo studies. J. Infect. Dis. **125:**486–490. http://dx.doi.org/10.1093/infdis/125.5.486.
49. **Kunst MW, Mattie H.** 1978. Cefazolin and cephradine: relationship between antibacterial activity in vitro and in mice experimentally infected with Escherichia coli. J. Infect. Dis. **137:**391–402. http://dx.doi.org/10.1093/infdis/137.4.391.
50. **Vella-Brincat JW, Begg EJ, Kirkpatrick CM, Zhang M, Chambers ST, Gallagher K.** 2007. Protein binding of cefazolin is saturable in vivo both between and within patients. Br. J. Clin. Pharmacol. **63:**753–757. http://dx.doi.org/10.1111/j.1365-2125.2006.02827.x.
51. **Craig WA, Welling PG, Jackson TC, Kunin CM.** 1973. Pharmacology of cefazolin and other cephalosporins in patients with renal insufficiency. J. Infect. Dis. **128**(Suppl)**:**S347–S353. http://dx.doi.org/10.1093/infdis/128.Supplement_2.S347.
52. **Ackerman BH, Taylor EH, Olsen KM, Abdel-Malak W, Pappas AA.** 1988. Vancomycin serum protein binding determination by ultrafiltration. Drug Intell. Clin. Pharm. **22:**300–303.
53. **Knudsen JD, Fuursted K, Espersen F, Frimodt-Moller N.** 1997. Activities of vancomycin and teicoplanin against penicillin-resistant pneumococci in vitro and in vivo and correlation to pharmacokinetic parameters in the mouse peritonitis model. Antimicrob. Agents Chemother. **41:**1910–1915.
54. **de Steenwinkel JE, Aarnoutse RE, de Knegt GJ, ten Kate MT, Teulen M, Verbrugh HA, Boeree MJ, van Soolingen D, Bakker-Woudenberg IA.** 2013. Optimization of the rifampin dosage to improve the therapeutic efficacy in tuberculosis treatment using a murine model. Am. J. Respir. Crit. Care Med. **187:**1127–1134. http://dx.doi.org/10.1164/rccm.201207-1210OC.
55. **Lee FH, Pfeffer M, Van Harken DR, Smyth RD, Hottendorf GH.** 1980. Comparative pharmacokinetics of ceforanide (BL-S786R) and cefazolin in laboratory animals and humans. Antimicrob. Agents Chemother. **17:**188–192. http://dx.doi.org/10.1128/AAC.17.2.188.
56. **Chapman SW, Steigbigel RT.** 1983. Staphylococcal beta-lactamase and efficacy of beta-lactam antibiotics: in vitro and in vivo evaluation. J. Infect. Dis. **147:**1078–1089. http://dx.doi.org/10.1093/infdis/147.6.1078.
57. **Healy DP, Polk RE, Garson ML, Rock DT, Comstock TJ.** 1987. Comparison of steady-state pharmacokinetics of two dosage regimens of vancomycin in normal volunteers. Antimicrob. Agents Chemother. **31:**393–397. http://dx.doi.org/10.1128/AAC.31.3.393.
58. **Forrest GN, Tamura K.** 2010. Rifampin combination therapy for nonmycobacterial infections. Clin. Microbiol. Rev. **23:**14–34. http://dx.doi.org/10.1128/CMR.00034-09.
59. **Jayaram R, Gaonkar S, Kaur P, Suresh BL, Mahesh BN, Jayashree R, Nandi V, Bharat S, Shandil RK, Kantharaj E, Balasubramanian V.** 2003. Pharmacokinetics-pharmacodynamics of rifampin in an aerosol infection model of tuberculosis. Antimicrob. Agents Chemother. **47:**2118–2124. http://dx.doi.org/10.1128/AAC.47.7.2118-2124.2003.
60. **Perlroth J, Kuo M, Tan J, Bayer AS, Miller LG.** 2008. Adjunctive use of rifampin for the treatment of Staphylococcus aureus infections: a systematic review of the literature. Arch. Intern. Med. **168:**805–819. http://dx.doi.org/10.1001/archinte.168.8.805.
61. **Reipert A, Ehlert K, Kast T, Bierbaum G.** 2003. Morphological and genetic differences in two isogenic Staphylococcus aureus strains with decreased susceptibilities to vancomycin. Antimicrob. Agents Chemother. **47:**568–576. http://dx.doi.org/10.1128/AAC.47.2.568-576.2003.
62. **Calvori C, Frontali L, Leoni L, Tecce G.** 1965. Effect of rifamycin on protein synthesis. Nature **207:**417–418. http://dx.doi.org/10.1038/207417a0.
63. **Campbell EA, Korzheva N, Mustaev A, Murakami K, Nair S, Goldfarb A, Darst SA.** 2001. Structural mechanism for rifampicin inhibition of bacterial RNA polymerase. Cell **104:**901–912. http://dx.doi.org/10.1016/S0092-8674(01)00286-0.
64. **Spelman D, Harrington G, Russo P, Wesselingh S.** 2002. Clinical, microbiological, and economic benefit of a change in antibiotic prophylaxis for cardiac surgery. Infect. Control Hosp. Epidemiol. **23:**402–404. http://dx.doi.org/10.1086/502074.
65. **Archer GL, Armstrong BC, Kline BJ.** 1982. Rifampin blood and tissue levels in patients undergoing cardiac valve surgery. Antimicrob. Agents Chemother. **21:**800–803. http://dx.doi.org/10.1128/AAC.21.5.800.
66. **Archer GL, Armstrong BC.** 1983. Alteration of staphylococcal flora in cardiac surgery patients receiving antibiotic prophylaxis. J. Infect. Dis. **147:**642–649. http://dx.doi.org/10.1093/infdis/147.4.642.
67. **Cirioni O, Mocchegiani F, Ghiselli R, Silvestri C, Gabrielli E, Marchionni E, Orlando F, Nicolini D, Risaliti A, Giacometti A.** 2010. Daptomycin and rifampin alone and in combination prevent vascular graft biofilm formation and emergence of antibiotic resistance in a subcutaneous rat pouch model of staphylococcal infection. Eur. J. Vasc. Endovasc. Surg. **40:**817–822. http://dx.doi.org/10.1016/j.ejvs.2010.08.009.